IGA of a Photocathode

Contents

1 200 kV Geometry **1**

1.1 Geometry . . . 1

1.2 Electric Field . . . 3

1.3 Optimization . . . 5

1.3.1 Volume Constraint . . . 5

1.3.2 Cost Function . . . 6

1.3.3 Additional Constraints . . . 6

1.3.4 NLopt . . . 6

1.3.5 Results . . . 6

1.4 Astra . . . 7

1 200 kV Geometry

1.1 Geometry

The 200 kV geometry was derived from version one of the CST model. Some simplifications were made such that the geometry may be considered rotationally symmetric. The dimensions of the electrode, puck, puck elevator, vacuum chamber and insulator were derived from the model as depicted in fig. 1. The boundary conditions remained the same, except for the increase in voltage, when compared to the 60 kV variant and the relative permittivity of the insulator was taken from the model to be 9.4.

The geometry is depicted in fig. 3. The numbers refer to the individual patches in the context of IGA. The patch boundaries are indicated by grey lines. The red lines represent homogeneous Dirichlet boundary conditions, the blue lines inhomogeneous Dirichlet boundary conditions with a value of -200 kV and the black lines indicate homogeneous Neumann boundaries. The patches containing insulator material are colored in red.

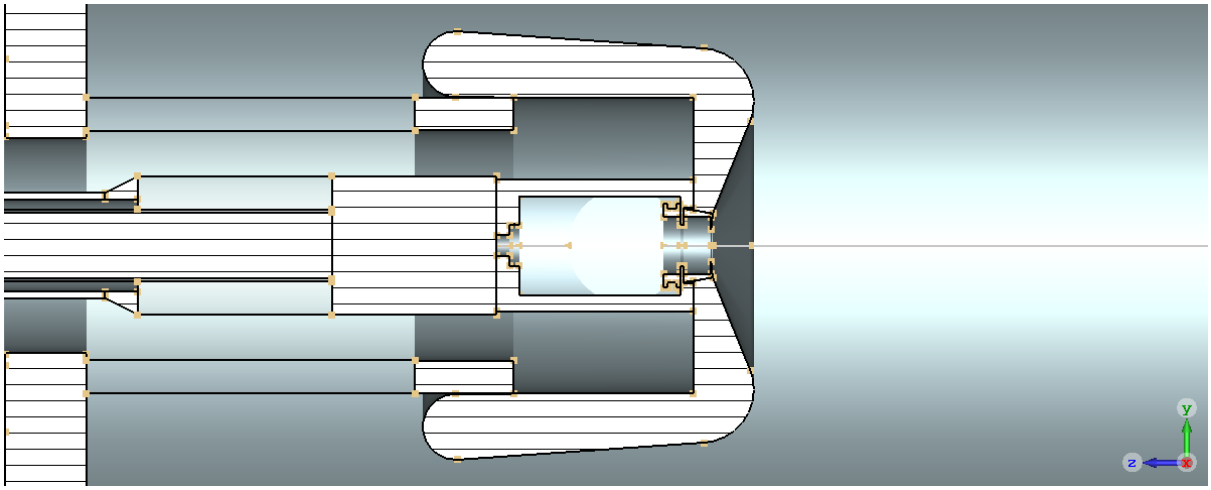

Figure 1: y-z view of the CST model for $x = 0$.

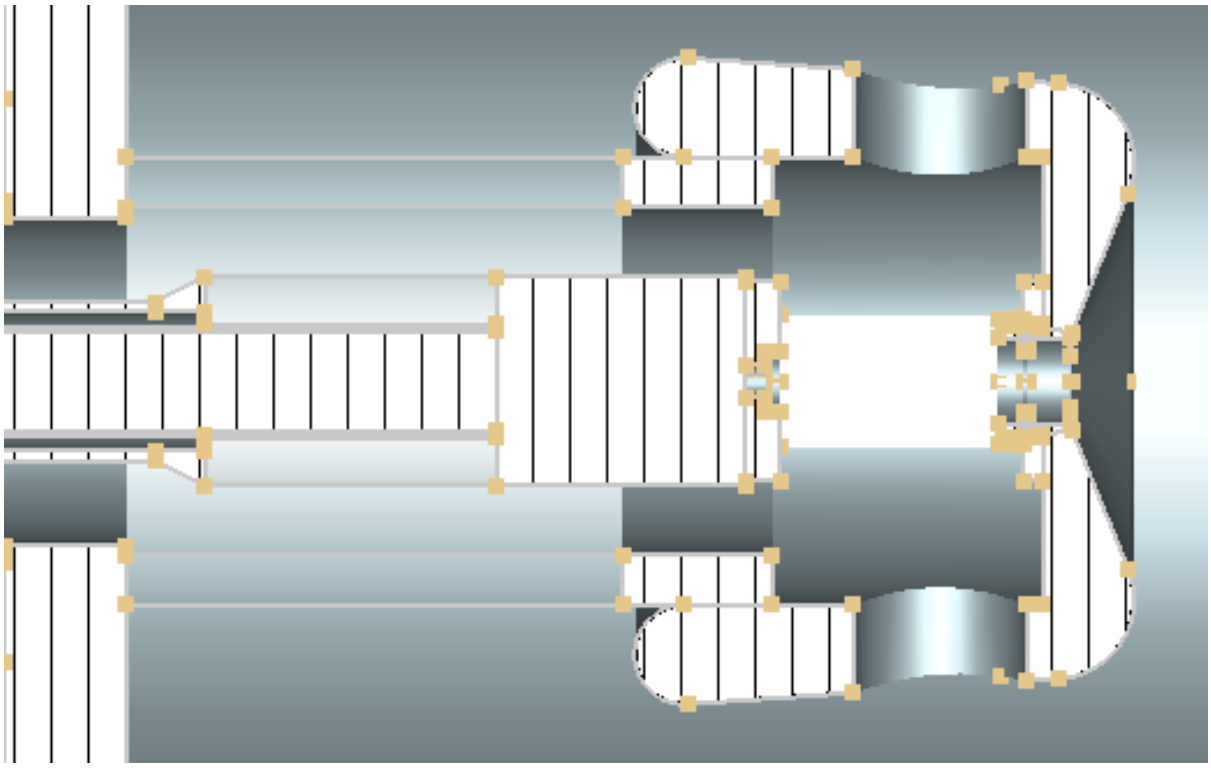

Figure 2: x-z view of the CST model for $y = 0$.

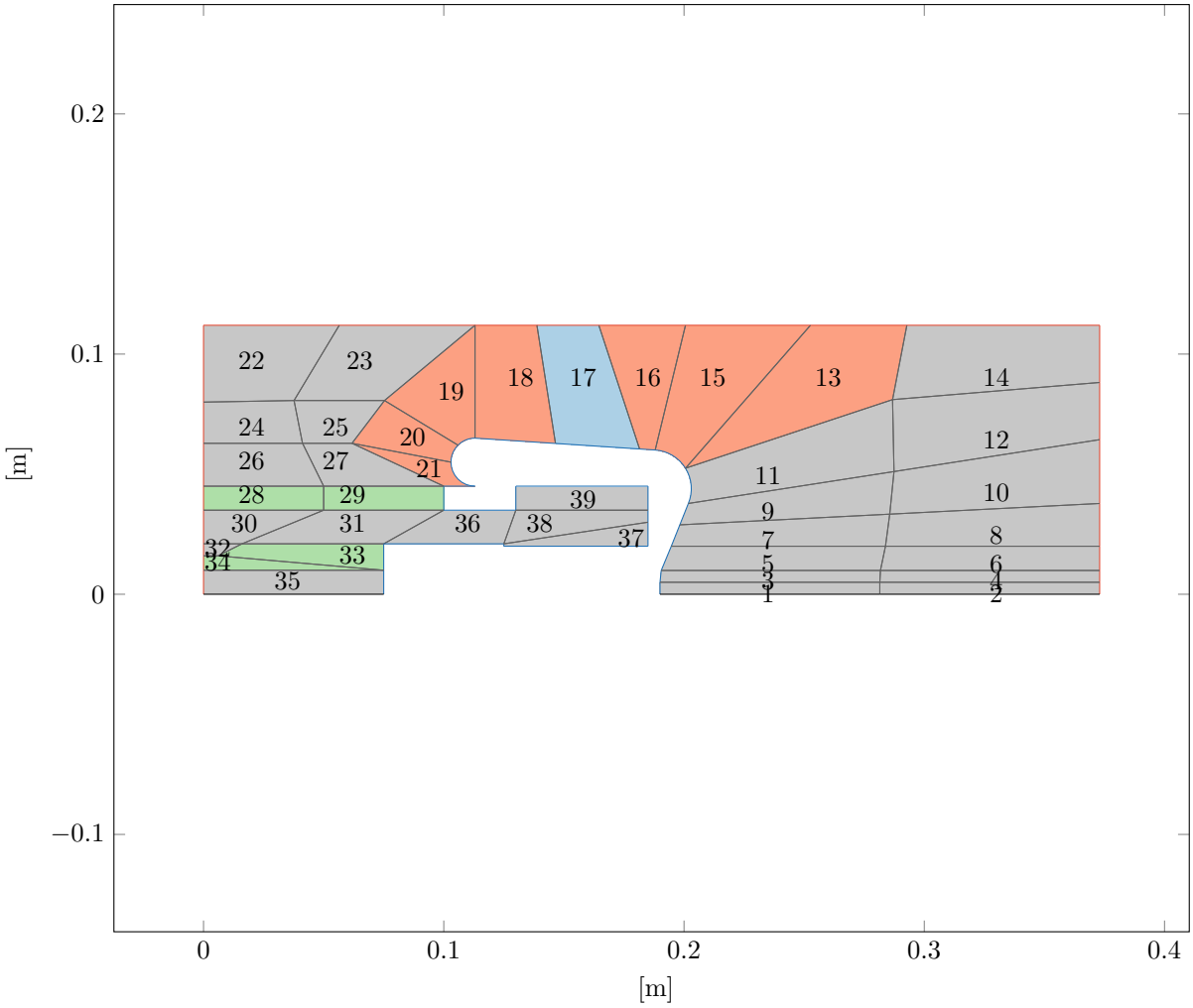

Figure 3: Refined 200 kV Photocathode geometry and boundary conditions.

1.2 Electric Field

The solution for the electric field is shown in fig. 4. It was computed with $p = 3$ as the degree of the basis functions and $n_{\text{sub}} = 128$ as the number of elements that each knot vector is uniformly split into. It is evident that there exist parts of the domain where the magnitude exceeds the limit of $10\,\frac{\text{MV}}{\text{m}}$. There are also very high gradients visible at the triple points however these also coincide with sharp corners so numerical issues might play a role.

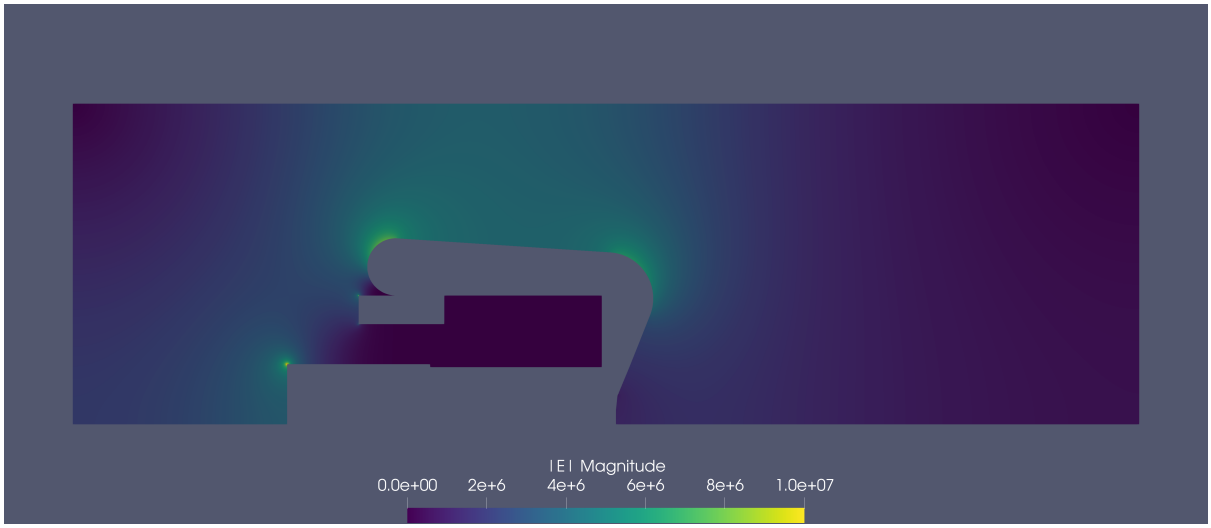

Figure 4: Absolute value of the electric field with $p = 3$ and $n_{\text{sub}} = 128$.

Additionally solutions with different degree and n_{sub} were performed to estimate the reliability of the results.

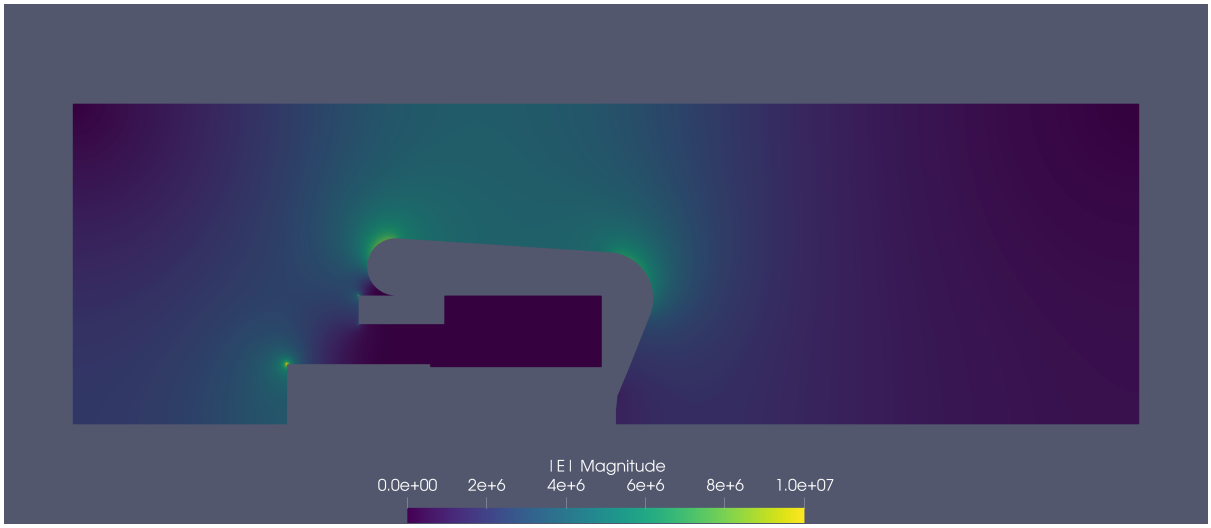

Figure 5: Absolute value of the electric field with $p = 2$ and $n_{\text{sub}} = 128$.

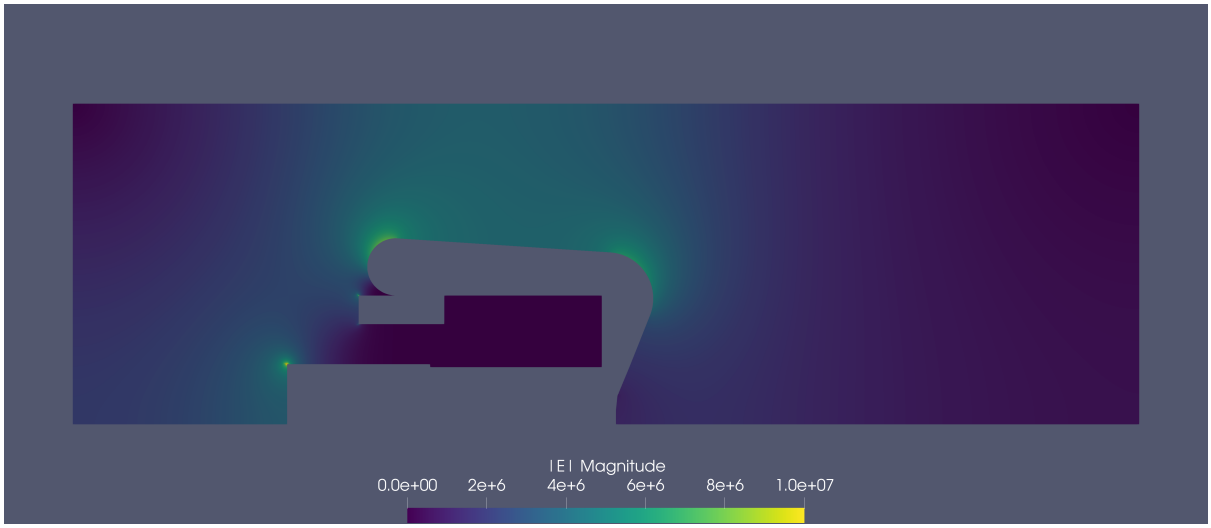

Figure 6: Absolute value of the electric field with $p = 2$ and $n_{\text{sub}} = 64$.

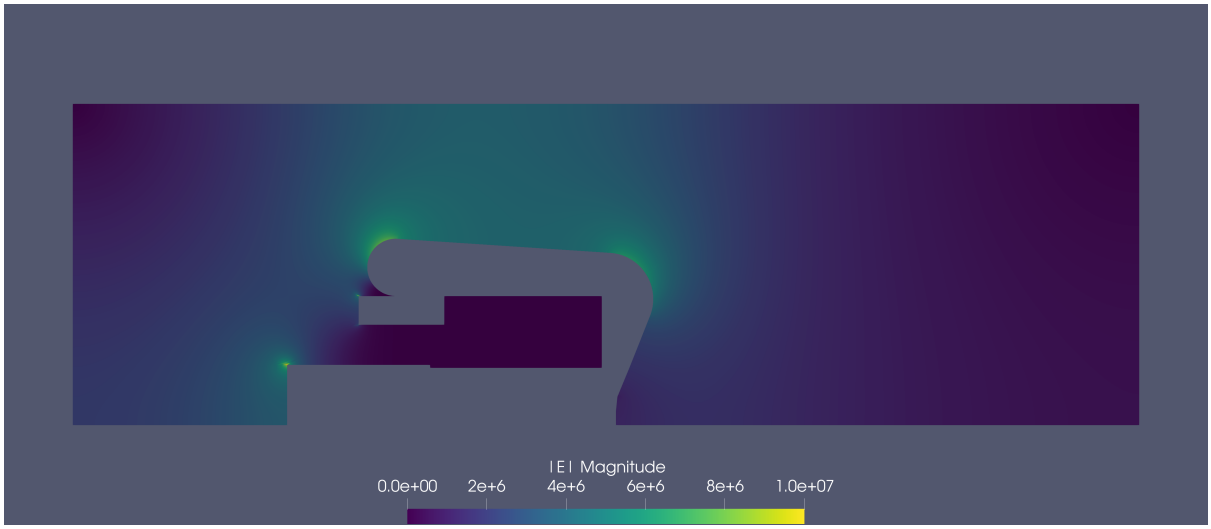

Figure 7: Absolute value of the electric field with $p = 2$ and $n_{\text{sub}} = 32$.

1.3 Optimization

The aim of the optimization will be to minimize the maximal field amplitudes. For practicality we will only look at the critical points of the geometry, i. e. the curvatures of the outer electrode and the triple points and average the field strengths over a given number of sample points. The lower part of the geometry will remain fixed so only the electrode boundaries of patches 15 through 21 from fig. 3 and their respective control points will be the DoFs. Another thing that might be considered is varying the length of the entire electrode. Aside from the fixed part of the geometry we also need to consider a volume constraint.

1.3.1 Volume Constraint

One of the constraints for the later optimization will be the weight of the electrode and thus its volume. We first compute the volume of the patches by taking into account the rotational symmetry and dis-

cretizing $V_{\text{ptc}} = \int_V r \, \mathrm{d}r \, \mathrm{d}\varphi \, \mathrm{d}z$ via numerical quadrature. We can then obtain the volume of the electrode by subtracting V_{ptc} from the cylinder formed by the vacuumchamber. We still need to consider the holes inside the electrode, visible in 2, and the correct lift geometry. The holes are computed by considering a cylinder with its height as a function of z. The curvature in x and y is disregarded, since it is the same for both coordinates. We can therefore determine the value by discretizing $V_h = \int_V \mathrm{d}x \, \mathrm{d}y \, \mathrm{d}z$. Lastly the white part below patches 22 and 37 already belongs to the lift and cable respectively and should therefore not be counted towards the volume of the electrode. The physical constraint is set at 625 cm^3 and the volume of the current geometry is computed as 613.6 cm^3.

1.3.2 Cost Function

- evaluates electric field in quadrature nodes and computes the average
- considers a given set of patches
- is based on the solution depicted in fig. 7
- current results indicate that it may be better to look at the maximum of the quadrature nodes

1.3.3 Additional Constraints

- upper and lower bounds are set for the control points
- the electrode's boundary from patch 15 to 21 is modeled as a single nurbs with C^1 continuity
- include the boundary of patch 11 as well?

1.3.4 NLopt

- implementation uses BOBYQA from the NLopt library
- many other derivative free algorithms can be tested in the same fashion

1.3.5 Results

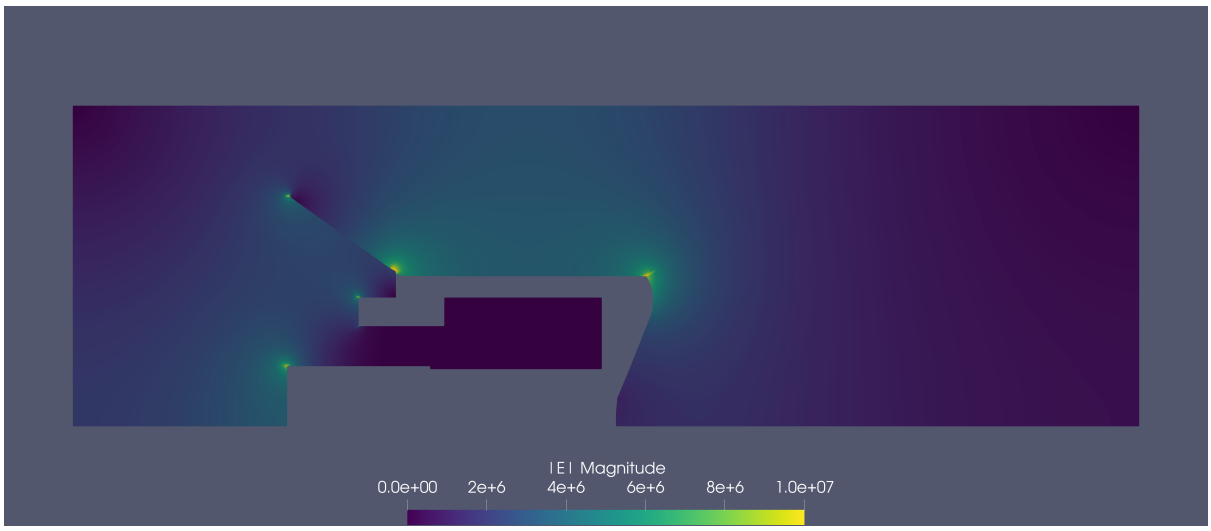

Figure 8: Optimization result using BOBYQA with the cost function evaluated in patches 13-21.

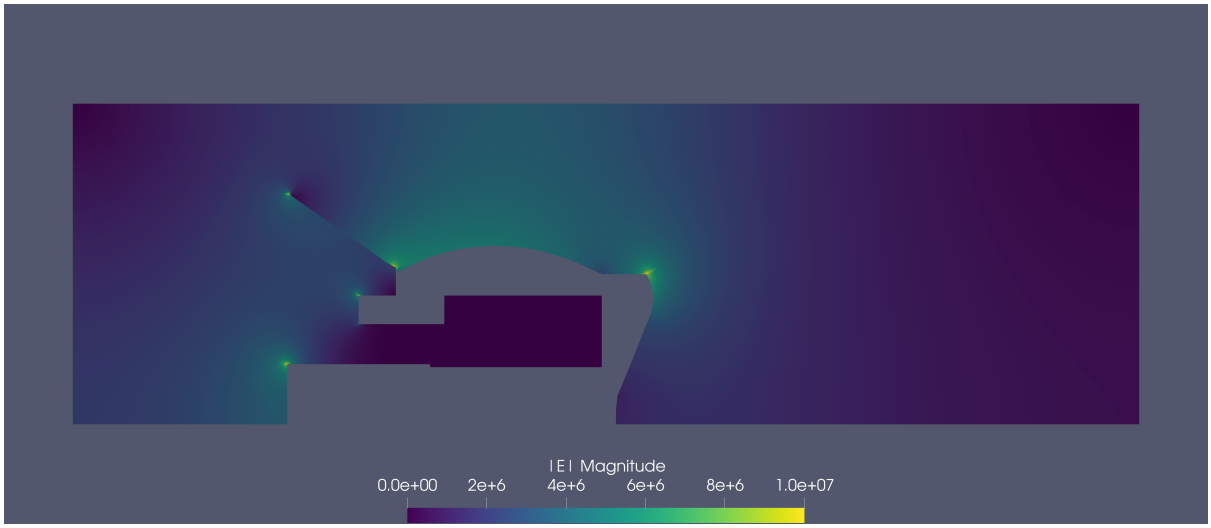

Figure 9: Optimization result using BOBYQA with the cost function evaluated in patches 13, 15 and 19, 20.

- minimizing the average seems to disregard the maximum values as indicated by the results

1.4 Astra

In the future we may also optimize the electrode boundary next to the puck, i. e. patches 3, 4 and 5 to obtain optimal particle trajectories. The cost function will be computed using Astra. (Perform all the tests for Astra also for the final Photocathode geometry?) The desired total bunch charge is 10 pC with a beam current of $(20 - 100)$ μA, whereas a typical value would be 100 fC. The bunch length is around 5 ps with a normalized transversal emittance of $e_{x,y} \leq 1$ mm mrad. The desired energy resolution is $\frac{\Delta E}{E} \leq 10^{-4}$. The tracking will be performed using individual bunches from a pulsed laser. The emission model may be derived from [3].

References

[1] Martin Espig. *Development, construction and characterization of a variable repetitive spin-polarized electron gun with an inverted-geometry insulator.* PhD thesis, Technische Universität Darmstadt, 2016.

[2] Vincent Wende. Simulations for investigation and improvements on a spinpolarized electron source with inverted-geometry insulator for the s-dalinac. Master's thesis, Technische Universität Darmstadt, 2017.

[3] Markus Wagner. *Production and investigation of pulsed electron beams at the S-DALINAC.* PhD thesis, Technische Universität Darmstadt, 2013.